AD-A195 045 AUTOIONIZATION FOR LOWER LEVEL DETRAPPING IN X-RAY LASERS(U) NAVAL RESEARCH LAB WASHINGTON DC R C ELTON 09 MAY 88 NRL-9103 1/1

UNCLASSIFIED F/G 9/3 NL

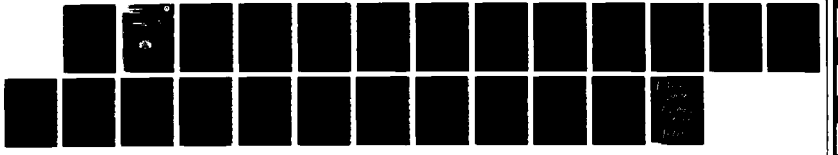

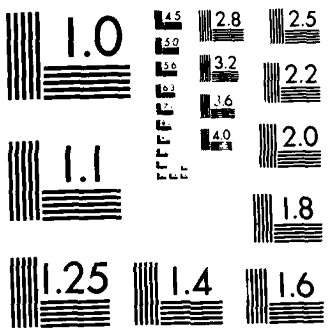

MICROCOPY RESOLUTION TEST CHART
NATIONAL BUREAU OF STANDARDS-1963-A

Laboratory

NRL Report 9103

Autoionization for Lower Level Detrapping in X-Ray Lasers

R. C. ELTON

Laser Plasma Branch
Plasma Physics Division

May 9, 1988

SECURITY CLASSIFICATION OF THIS PAGE

REPORT DOCUMENTATION PAGE

1a. REPORT SECURITY CLASSIFICATION UNCLASSIFIED	1b. RESTRICTIVE MARKINGS
2a. SECURITY CLASSIFICATION AUTHORITY	3. DISTRIBUTION / AVAILABILITY OF REPORT Approved for public release; distribution unlimited.
2b. DECLASSIFICATION / DOWNGRADING SCHEDULE	
4. PERFORMING ORGANIZATION REPORT NUMBER(S) NRL Report 9103	5. MONITORING ORGANIZATION REPORT NUMBER(S)
6a. NAME OF PERFORMING ORGANIZATION Naval Research Laboratory 6b. OFFICE SYMBOL (If applicable) Code 4733	7a. NAME OF MONITORING ORGANIZATION
6c. ADDRESS (City, State, and ZIP Code) Washington, DC 20375-5000	7b. ADDRESS (City, State, and ZIP Code)
8a. NAME OF FUNDING / SPONSORING ORGANIZATION Strategic Defense Initiative Organization 8b. OFFICE SYMBOL (If applicable)	9. PROCUREMENT INSTRUMENT IDENTIFICATION NUMBER
8c. ADDRESS (City, State, and ZIP Code)	10. SOURCE OF FUNDING NUMBERS PROGRAM ELEMENT NO. 5611-53N; PROJECT NO. RR011-09-41; TASK NO.; WORK UNIT ACCESSION NO.

11. TITLE (Include Security Classification)
Autoionization for Lower Level Detrapping in X-Ray Lasers

12. PERSONAL AUTHOR(S)
Elton, R. C.

13a. TYPE OF REPORT	13b. TIME COVERED	14. DATE OF REPORT (Year, Month, Day)	15. PAGE COUNT
Interim	FROM _____ TO _____	1988 May 9	24

16. SUPPLEMENTARY NOTATION

17. COSATI CODES			18. SUBJECT TERMS (Continue on reverse if necessary and identify by block number)
FIELD	GROUP	SUB-GROUP	

19. ABSTRACT (Continue on reverse if necessary and identify by block number)

A novel type of X-ray laser is analyzed in which the population of the lower level is depleted by autoionization instead of by spontaneous decay. The intention is to decrease radiative trapping effects that quench the gain and require microscopic plasmas. Proof-of-principle atomic-physics experiments and numerical modeling are needed to verify predicted feasibility, fluorescence, and lasing.

20. DISTRIBUTION / AVAILABILITY OF ABSTRACT ☐ UNCLASSIFIED/UNLIMITED ☐ SAME AS RPT. ☐ DTIC USERS	21. ABSTRACT SECURITY CLASSIFICATION UNCLASSIFIED
22a. NAME OF RESPONSIBLE INDIVIDUAL Raymond C. Elton	22b. TELEPHONE (Include Area Code) (202)-767-2754 22c. OFFICE SYMBOL Code 4733

DD FORM 1473, 84 MAR 83 APR edition may be used until exhausted. All other editions are obsolete.

SECURITY CLASSIFICATION OF THIS PAGE

CONTENTS

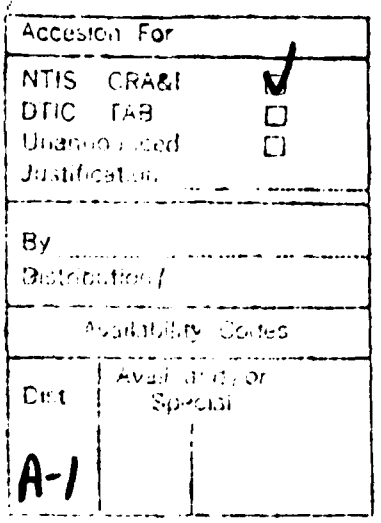

AUTOIONIZATION FOR LOWER LEVEL DETRAPPING IN X-RAY LASERS

INTRODUCTION

The trapping of radiation resulting from lower laser level decay is a major problem in research for extending plasma X-ray lasers to wavelengths shorter than 100 Å at high output power [1,2]. Besides the limitation on gain brought about by the reduced radiative depopulation of this level, the required micrometer-scale diameter presents severe experimental difficulties. A novel scheme [1-3] intended to reduce this trapping is shown in the energy level diagram of Fig. 1. Here the lower laser level autoionizes at a rate exceeding that for spontaneous emission, thus depleting the lower level population by electron emission instead of (trapped) spontaneous photon emission. This constitutes a different class of lasers than presently pursued. The upper laser level has to be fairly stable against autoionization and would most likely be pumped by a resonant photon from a nearby ion in a "flash-lamp" concept. This scheme requires a two-component plasma with an accurate wavelength match for resonance-excitation pumping. Promising ion candidates based on limited existing information are identified here. The need for expanded experimental and theoretical data bases as guidance for numerical modeling of specific combinations, as well as definitive gain calculations and experiments in nonequilibrium plasmas, are emphasized.

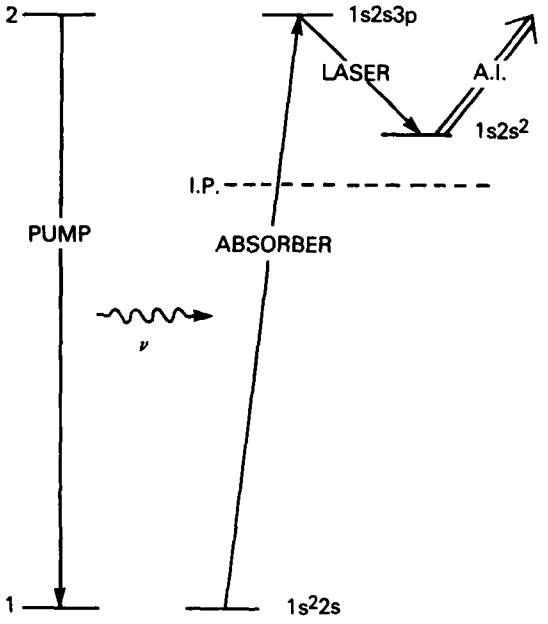

Fig. 1 — Detrapping concept using autoionization (A.I.) on levels above the ionization potential (I.P.) to directly deplete the lower laser level population, shown here as $1s2s^2$

Manuscript approved November 6, 1987.

ANALYSIS

Decay Rates

As a guideline for the analysis that follows, we use a set of selection criteria in three steps, initially ignoring any consideration of how the autoionization levels are pumped to inversion, and require that:

1. excitation (and innershell vacancy) be limited to a single electron;
2. the lower laser level decay predominantly by autoionization;
3. the upper laser level be relatively stable against autoionization; and
4. the laser line-width be limited to Doppler broadening (for maximum gain).

We further limit the analysis to matched-line resonance photoexcitation pumping and require as additional criteria:

5. an intense pumping line,
6. a good energy resonance between the pumping (p) and absorbing (a) transitions; and
7. a high line strength (A_a) for the absorbing transition.

For maximum gain and output, we further require:

8. a strong (A_L) lasing transition;
9. lack of absorption of the laser emission by other lines; and
10. p,a atomic species of similar Z, for congruent/adjacent plasmas.

The first criterion essentially eliminates He-like ions that require double excitation of two electrons to reach the autoionization levels. The next simplest system is the Li-like, three-electron isoelectronic sequence (analyzed here). Figure 1 shows one transition as an example. Here, lasing takes place on a 3-2 transition at a wavelength and with a gain close to those of the Balmer-α lines of hydrogenic and He-like species. The lasing wavelengths (λ_L) may be estimated empirically by

$$\lambda_L = 6300/(Z - 1.7)^2 \text{ Å}, \quad (1)$$

or ~ 118 Å for fluorine (Z = 9). This is plotted in Figs. 2 and 3.

The second criterion minimizes radiative trapping and maximizes autoionization from the lower laser level. The third criterion permits a population inversion that is not reduced by autoionization from the upper level. This third condition does not conflict with the second, since the autoionization rate decreases with principal quantum number n as $1/n^3$. Criteria 5 through 7 refer to efficient matched-line photon pumping of a high population-density inversion by resonance transitions such as 2-1 in H- or He-like ions. Criteria 8 and 9, along with criteria 4, maximize the laser output by also minimizing losses.

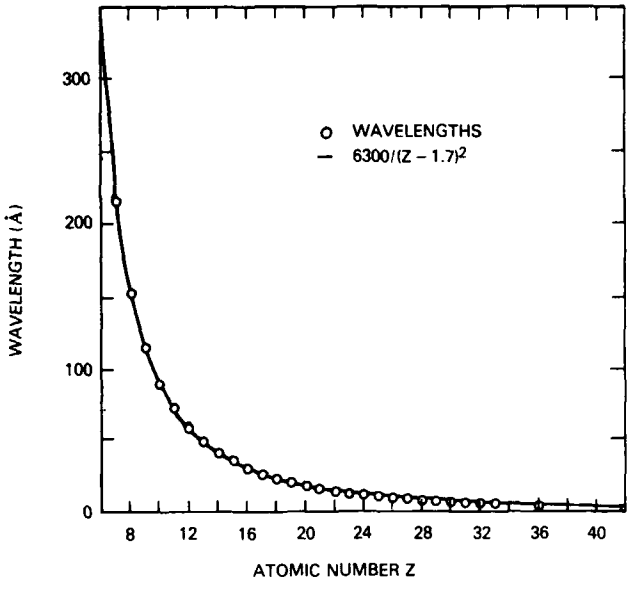

Fig. 2 — Wavelengths for 3-2 doubly excited transitions in Li-like ions vs atomic number Z

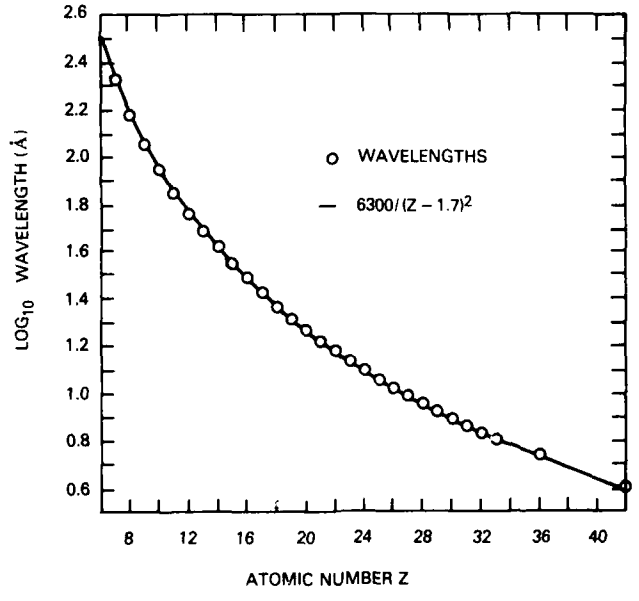

Fig. 3 — Log_{10} of wavelengths for 3-2 doubly excited transitions in Li-like ions vs atomic number Z

For our analysis, we have relied on the theoretical calculations of Vainshtein and Safronova [4] and more recently by Chen [5]. A check for the important transitions here (Table 1) for Z = 26 shows that wavelengths (transition energies) in these two references agree to within ~0.04% and are therefore used almost interchangeably, as discussed below in regard to Table 2. This wavelength precision agrees with the ±0.5 mÅ estimate for Z = 26 of Bely-Dubau et al [6] The theoretical radiative rates for these cases appear to agree within ~4%, which is better than the overall estimate of ~15% given by Chen [5]. Either source is entirely adequate—we use those by Chen for convenience. The autoionization rates are a different story, however. Here differences can be several orders of magnitude. Given some glaring inconsistencies in Ref. 4 in this regard (as pointed out by Chen [5]), we use Chen's values here.

Table 1 — Summary of Z-Dependence for Criteria 1 through 4

Lower Lasing	Upper Lasing	Z_{min}	Z_{max}
$1s2s^2\ {}^2S$ (F)	$1s2s3p\ {}^2P_{1/2,3/2}$ (J)	12	30
$1s2s2p\ {}^2P_{1/2}$ (G)	$\{1s2s3d\ {}^2D_{3/2}\}^*$ (K)	8	16
	$1s2p3p\ {}^2S_{1/2}$ (M_S)	12	16
	$1s2p3p\ {}^2P_{1/2,3/2}$ (M_P)	8	16
	${}^2D_{3/2}$ (M_D)	16	16
${}^2P_{3/2}$ (G)	$\{1s2s3d\ {}^2D_{3/2,5/2}\}$ (K)	8	36
	$1s2p3p\ {}^2S_{1/2}$ (M_S)	12	36
	${}^2P_{1/2,3/2}$ (M_P)	8	36
	${}^2D_{3/2,5/2}$ (M_D)	16	36
$1s2p^2\ {}^2S_{1/2}$ (H)	$\{1s2p3s\ {}^2P_{1/2,3/2}\}$ (L_P)	15	16
	$\{1s2p3d\ {}^2P_{1/2,3/2}\}$ (N_P)	15	16
${}^2D_{3/2,5/2}$ (H)	$\{1s2p3s\ {}^2P_{1/2,3/2}\}$ (L_P)	15	16
	$\{1s2p3d\ {}^2P_{1/2,3/2}\}$ (N_P)	15	16
	${}^2D_{3/2,5/2}\}$ (N_D)	15	16
	${}^2F_{5/2,7/2}\}$ (N_F)	15	16

*Lunney [3]

Criterion 1: Beginning with criteria 1 through 4, the simplest example satisfying criterion 1 is the Li-like three-electron isoelectronic sequence with a 1s vacancy, i.e., with $1s2\ell 3\ell''$ and $1s2\ell 2\ell'$ upper and lower lasing states, respectively (ℓ,ℓ' = s,p and ℓ'' = s,p,d).

Criterion 2: This condition specifies that the lower laser level autoionization rate be at least five times the radiative rate and sets the first upper bound on Z for all three possible lower laser states, i.e.,

$1s2s^2$	$Z < 30$	(shown in Fig. 4)
$1s2s2p\ {}^2P_{1/2}$	$Z < 16$	(shown in Fig. 5)
$1s2s2p\ {}^2P_{3/2}$	$Z < 36$	(shown in Fig. 6)
$1s2p^2$	$Z < 16$	(shown in Fig. 7).

Table 2 — Possible Matches

Z_p	λ_p (Å)	Z_a	λ_a (Å)	$\Delta\lambda/\lambda$ ($\times 10^4$)	$Trans_a$	A_a/A_{He}* (10^{13} s^{-1})
Lyman-α Pump						
9	14.9823(S)[a]	9	14.9822[b]	0.13	A-J	0.07
		9	14.9825[b]	0.33	A-J	0.07
9	14.9877(W)[a]	9	14.9822[b]	3.9	A-J	0.07
		9	14.9825[b]	3.7	A-J	0.07
9	14.8823(S)[a]	9	14.990[c]	5.3	$B\text{-}M_D$	0.09
	14.9877(W)[a]	9		1.3	$B\text{-}M_D$	0.09
21	2.7360(S)[a]	20	2.7333[c]	9.9	A-J	0.06
36			no match			
	0.82712(W)[a]	36	no match			
44	0.60763(S)[a]	42	no match			
	0.61309(S)[a]	42	no match			
Helium-α Pump						
16	5.0389[d]	15	5.0380[c]	1.0	B-M	0.05
			5.0409[c]	4.8	B-M	0.04
28	1.5885[d]	26	1.5884[b]	0.63	$B\text{-}M_P$	0.006
			1.5884[b]	0.63	$B\text{-}M_D$	0.0002
			1.5858[b]	17	A-J	0.082
			1.5869[b]	10	A-J	0.085
29	1.4777[d]	27	1.4773[c]	2.7	$B\text{-}K_D$	0.0008
39	0.80094[d]	36	no match			
45	???	42				

[a]See Ref. 9; [b] see Ref. 5; [c]see Ref. 4; [d]see Ref. 10.

*Note that division by A_{He} in column 7 normalizes the absorption figure of merit to the He-like $1s3p\,^1P\text{-}1s^2$ transition.

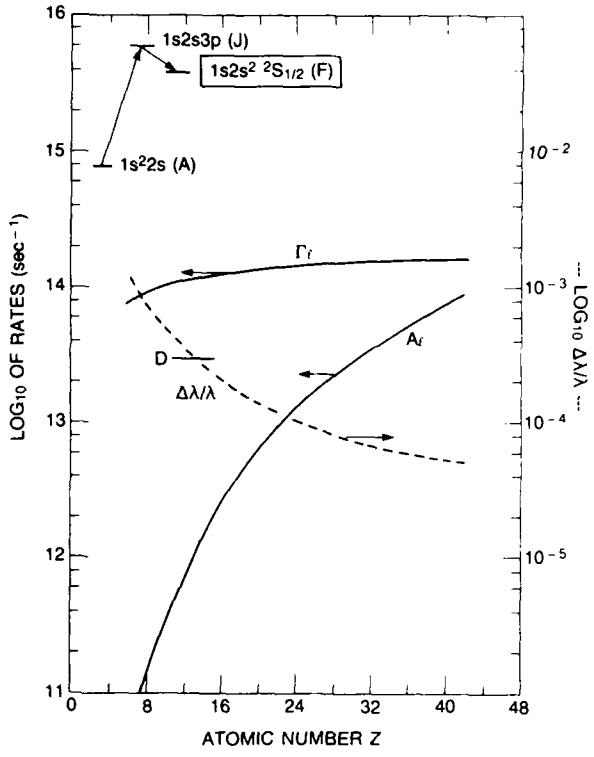

Fig. 4 — Autoionization rates (Γ_ℓ) and radiative decay rates (A_ℓ) for a $1s2s^2$ lower laser configuration vs atomic number Z

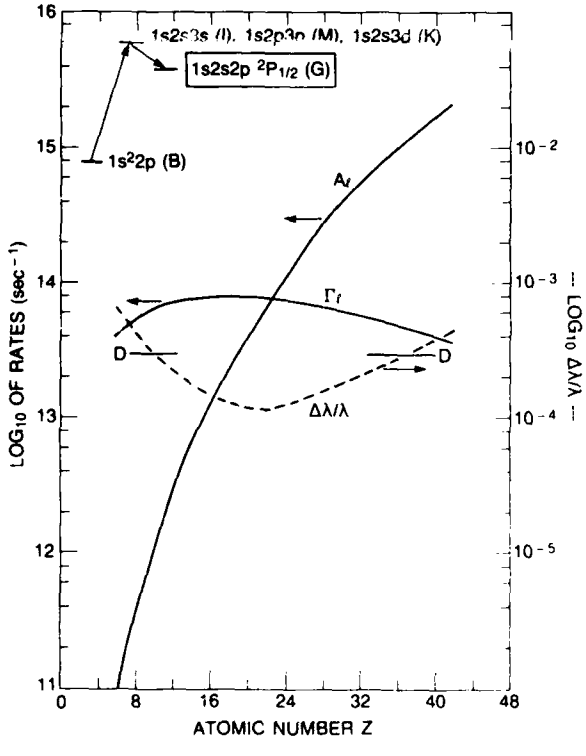

Fig. 5 — Autoionization rates (Γ_ℓ) and radiative decay rates (A_ℓ) for a $1s2s2p\ ^2P_{1/2}$ lower laser term vs atomic number Z

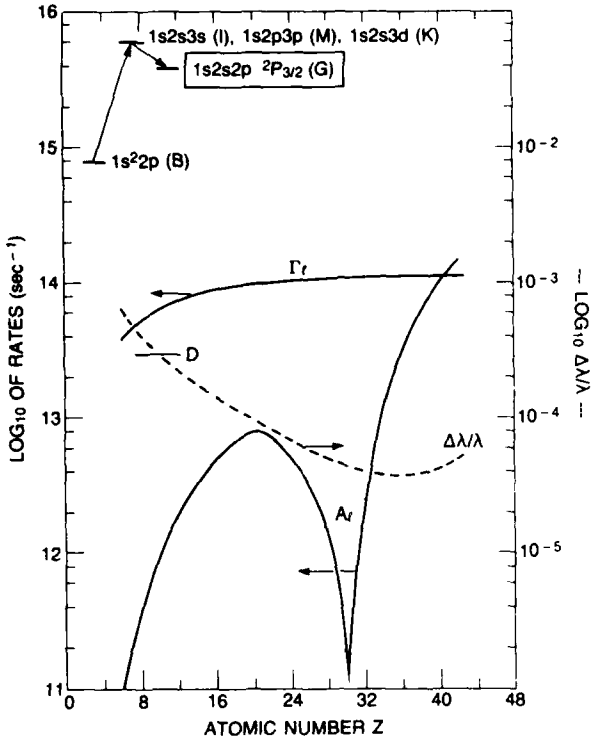

Fig. 6 — Autoionization rates (Γ_ℓ) and radiative decay rates (A_ℓ) for a 1s2s2p $^2P_{3/2}$ lower laser term vs atomic number Z

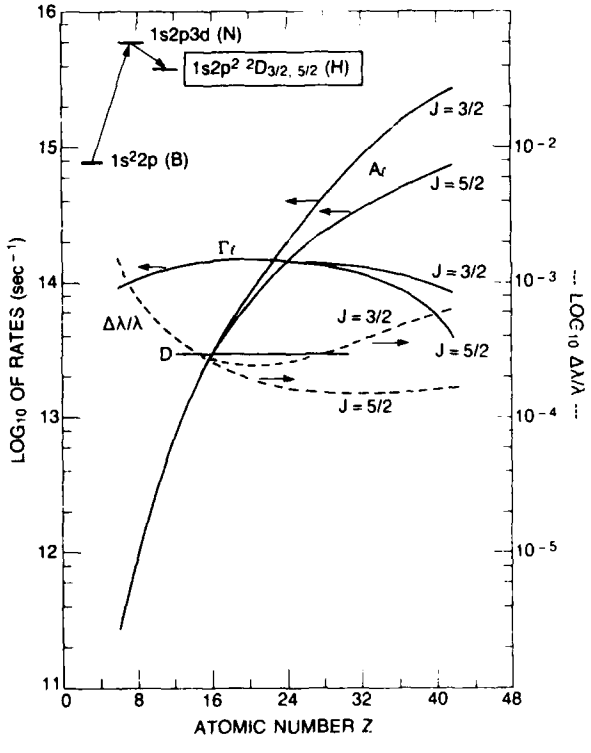

Fig. 7 — Autoionization rates (Γ_ℓ) and radiative decay rates (A_ℓ) for 1s2p^2 $^2D_{3/2,5/2}$ lower laser terms vs atomic number Z

(In Fig. 6, the dip in A_ℓ to a minimum for J = 3/2 at Z = 30 is due to a strong cancellation in the matrix elements [7], and the true bound is dependent on the collisional mixing with J = 1/2 terms (Fig. 4).)

Criterion 3: Next, relating these three lower laser level possible configurations to criterion 3 for the upper laser level, we require an upper level radiative rate at least as large as its autoionization rate. Note that the first lower level option ($1s2s^2$) requires a 1s2s3p upper laser level configuration, for which autoionization rates become less than radiative decay rates for Z > 8 (see Fig. 8). The second lower level choice, 1s2s2p, may combine with either a 1s2s3s, a 1s2s3d, or a 1s2p3p upper configuration (see Figs. 9 through 11). For the first (single) 1s2s3s $^2S_{1/2}$ term of these three, criterion 3 is satisfied for Z > 24 (Fig. 9). For the second upper level choice, 1s2s3d $^2D_{3/2,5/2}$, criterion 3 is met for all Z (Fig. 10). For the third choice, 1s2p3p, the $^2S_{1/2}$ terms are satisfactory for Z > 12 (Fig. 11); the $^2D_{3/2,5/2}$ are suitable for Z > 16 (Fig. 12); and the $^2P_{1/2,3/2}$ terms are very stable against autoionization for all Z's by selection rules and are not plotted. Concerning the third possible lower laser level, $1s2p^2$, upper terms such as 1s2p3s $^2P_{1/2,3/2}$ satisfy criterion 3 for Z > 12 (Fig. 13). In the 1s2p3d configuration, the $^2P_{1/2,3/2}$ terms obey criterion 3 for all Z's considered (Fig. 14), while the $^2D_{3/2,5/2}$ terms obey criterion 3 by a ratio of at least 3 orders of magnitude and are not plotted (but again are limited to Z ≤ 16 according to criterion 2); for the $^2F_{5/2,7/2}$ terms, criterion 3 is obeyed for Z > 12 (Fig. 15).

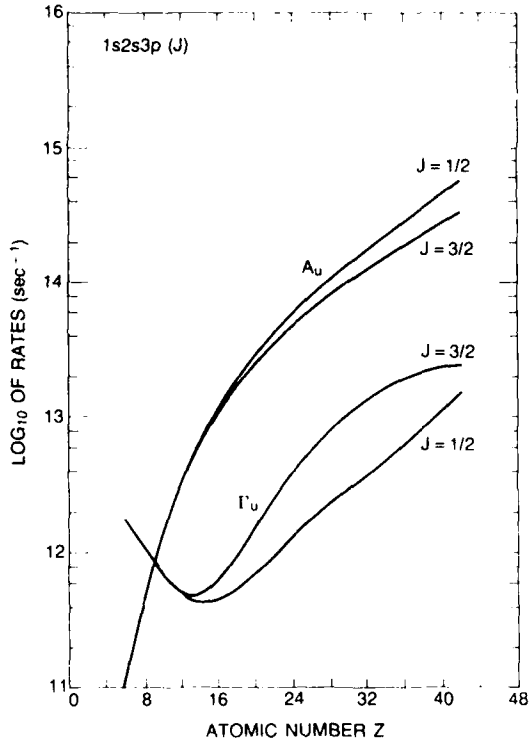

Fig. 8 — Autoionization rates (Γ_u) and radiative decay rates (A_u) for a 1s2s3p upper laser configuration vs atomic number Z

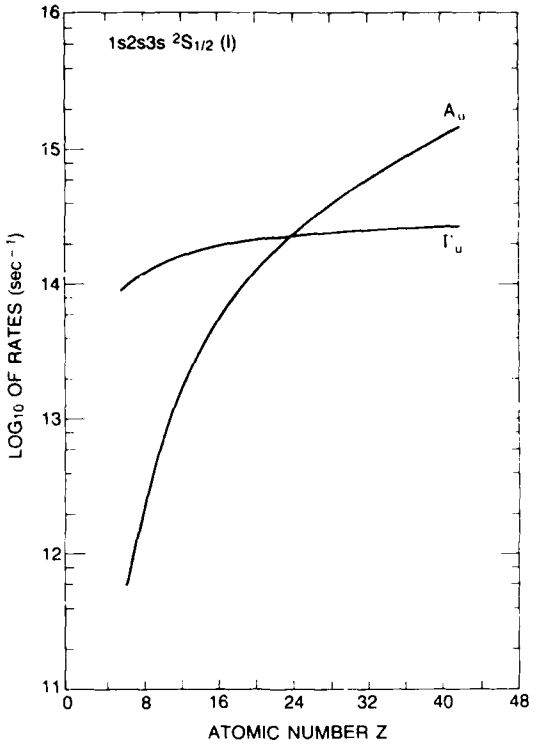

Fig. 9 — Autoionization rates (Γ_u) and radiative decay rates (A_u) for a 1s2s3s $^2S_{1/2}$ upper laser term vs atomic number Z

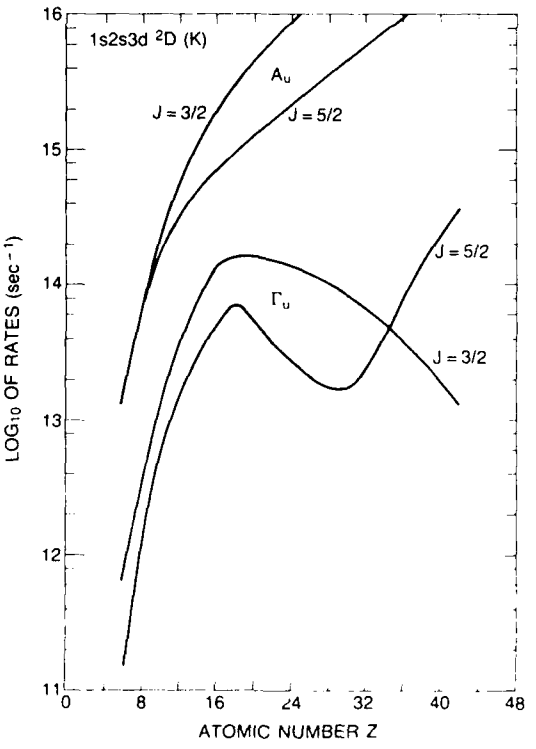

Fig. 10 — Autoionization rates (Γ_u) and radiative decay rates (A_u) for 1s2s3d $^2D_{3/2,5/2}$ upper laser terms vs atomic number Z

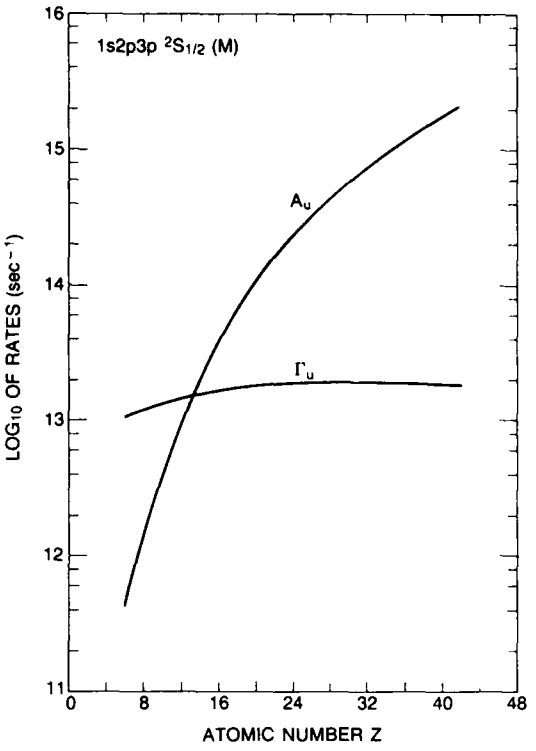

Fig. 11 — Autoionization rates (Γ_u) and radiative decay rates (A_u) for a 1s2p3p $^2S_{1/2}$ upper laser term vs atomic number Z

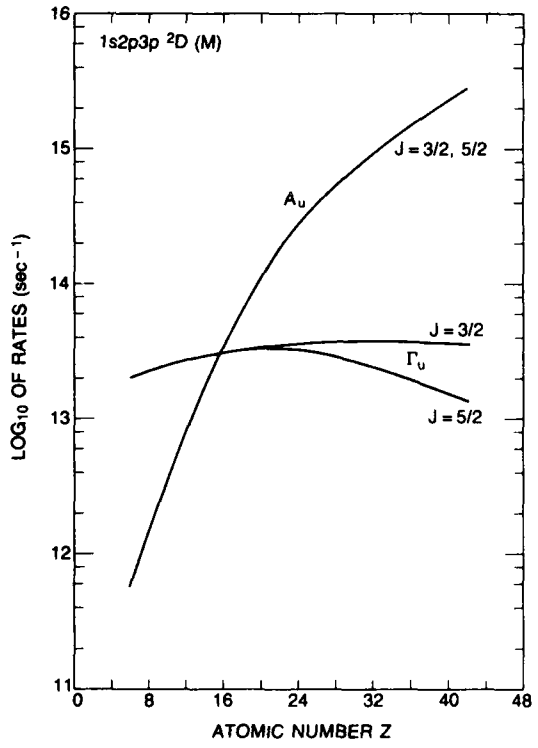

Fig. 12 — Autoionization rates (Γ_u) and radiative decay rates (A_u) for 1s2p3p $^2D_{3/2,5/2}$ upper laser terms vs atomic number Z

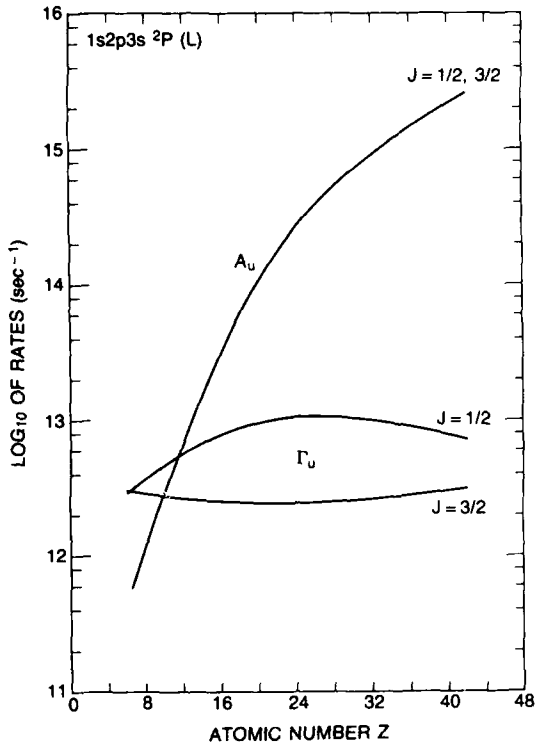

Fig. 13 — Autoionization rates (Γ_u) and radiative decay rates (A_u) for 1s2p3s $^2P_{1/2,3/2}$ upper laser terms vs atomic number Z

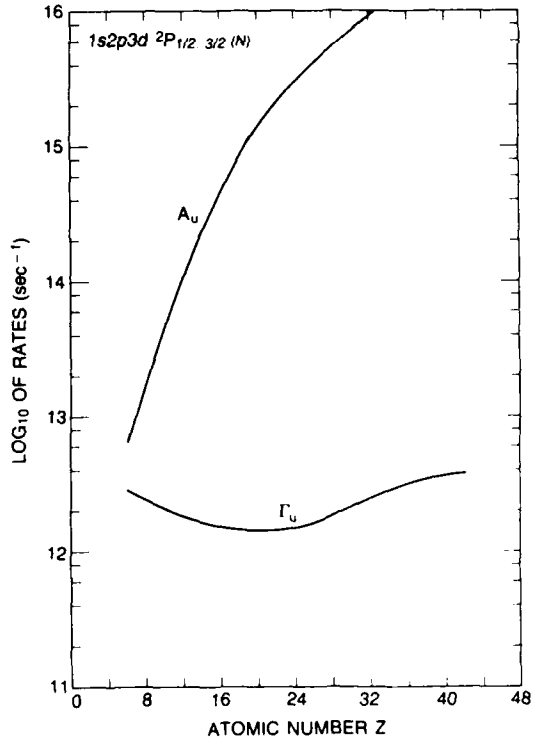

Fig. 14 — Autoionization rates (Γ_u) and radiative decay rates (A_u) for 1s2p3d $^2P_{1/2,3/2}$ upper laser terms vs atomic number Z

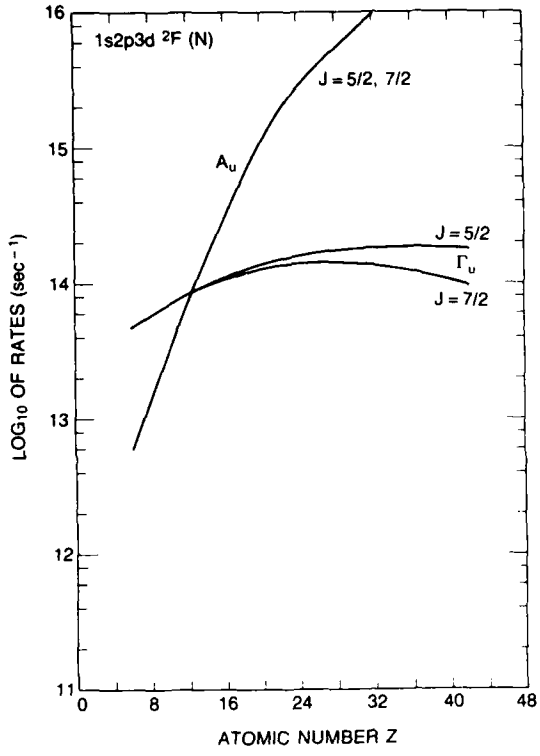

Fig. 15 — Autoionization rates (Γ_u) and radiative decay rates (A_u) for 1s2p3d $^2F_{5/2,7/2}$ upper laser terms vs atomic number Z

Criterion 4: The natural width of the laser line can be approximated by $\Delta\nu = (A_\ell + \Gamma_\ell)/2\pi$ (in frequency units) for the lower laser level radiative (A_ℓ) and autoionization (Γ_ℓ) decay rates that dominate those of the upper laser level. The ratio $\Delta\nu/\nu_L$ (where ν_L is the frequency of a typical laser transition) is plotted in Figs. 4 through 7 and decreases with increasing Z. When this is equated to a typical corresponding Doppler broadening ratio [8] of $\sim 3 \times 10^{-4}$, it provides additional limits for Z according to criterion 4 above. This is noted by D-markers in Figs. 4 through 7.

A summary of criteria 1 through 4, based on liberal interpretation of Figs. 4 through 15, results in Table 1 for LS-coupled transitions. The configuration representations in parentheses are those chosen by Chen [5], with subscripts added to show the L-values. This labeling also provides brevity in Table 2. (No distinction is made for singlet or triplet parentage because collisional mixing is expected at the densities involved in X-ray lasers.)

The brackets {....} in Table 1 represent levels that are not reached directly by single-electron electric dipole transitions from $1s^22s$ (A) or $1s^22p$ (B) lower configurations. This slightly violates the first criterion and also violates criterion 7 for a strong absorption (i.e., the transition probability is ~ 10 times lower than for single-electron transitions). Note that $1s2p^2\ ^2S_{1/2}$ - $1s2p3d\ ^2D_{3/2}$ are ruled out by the ΔL selection rule. Hence, the most promising transitions are reduced to six upper level terms.

Line Matching for Photon Pumping

Criteria 5 and 6: Criterion 5 now requires that pumping of population density in the upper laser level be by photon absorption from an intense line source. For this we choose n = 2-1 resonance

lines of hydrogenic and He-like ions and search for good line matches within the widths of the emitting and absorbing transitions (criterion 6). The absorbing transition will be Doppler broadened according to criterion 3, as will the pumping transition except for some possible additional opacity broadening. (This would help achieve a good match but would decrease the overall system efficiency.) Again, for Doppler broadening, we expect $\Delta\lambda/\lambda \approx 3 \times 10^{-4}$. In searching for wavelength matches, theoretical data of Vainshtein and Safronova [4] and Chen [5] are used. For this purpose they agree within $\Delta\lambda/\lambda \approx 4 \times 10^{-4}$ for Z = 26 for the important transitions given above; this is about the Doppler spread expected. We have chosen the closest match in each case for Table 2 and labeled them by superscripts, without precise measurements not knowing which of the two is the most accurate.

As a first estimate of possible matches, we can plot $\Delta\lambda/\lambda$ vs the nuclear charge Z of the pumping ion and Z+1, Z, Z-1, Z-2, and Z-3 for the Li-like absorbing ions. For this, we limit the pumping transitions to hydrogenic Lyman-α (Figs. 16 through 19) and He-like 2-1 "alpha" (Figs. 20 through 23). These lines are typically the most intense in the very short wavelength region for a particular element.

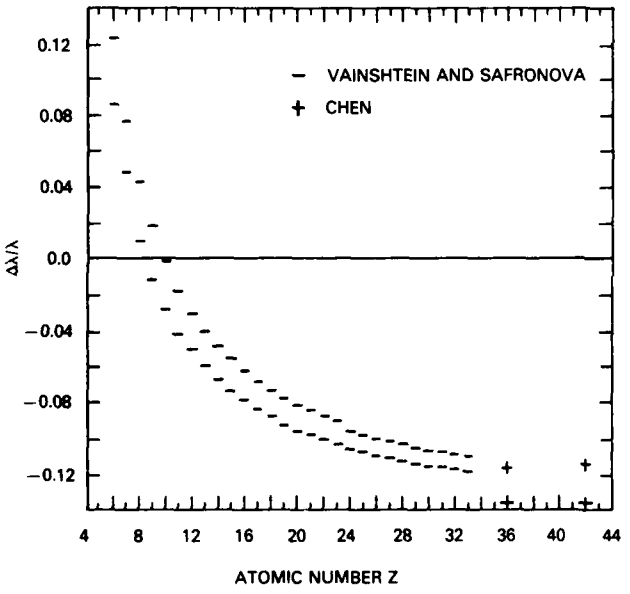

Fig. 16 — Line-matching factor for a Lyman-α pump line from an ion of atomic number Z and a Li-like absorber of the same Z

In Figs. 16 through 23, the dashed markers indicate the upper and lower bounds for all of the listed Li-like innershell transitions. For example, Fig. 16 shows a match between Lyman-α of hydrogenic fluorine (Z = 9) and Li-like fluorine (actually the only match with the same Z, which is a decided advantage in a single-element plasma). Likewise, Fig. 17 shows a possible match for Z = 22 with perhaps Z = 21 or Z = 23. Possible matches for He-like pump ions include Z = 16, 28, and 29 (Figs. 21 through 22). We now explore these possible matches further and attempt to satisfy the remaining criteria while satisfying the guidelines in Table 1.

One of the most promising matches for a Lyman-α pump line is Z = 9 pump (p) and absorber (a) ions, as shown in the first example in Table 2. This does, however, violate criterion 4 above, which determined Z_{min} = 12 for a J level, and therefore leads to a slightly reduced gain coefficient. Note that two sets of values for Z = 9 are given for two possible matches, depending on the source of data. Also, the data used here [4,5] indicate no match for the transition suggested by Lunney [3] (footnote in Table 1 here).

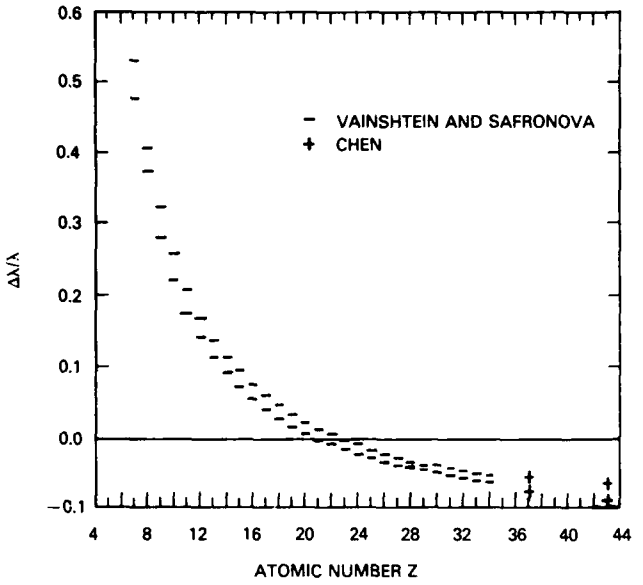

Fig. 17 — Line-matching factor for a Lyman-α pump line from an ion of atomic number Z and a Z-1 Li-like absorber

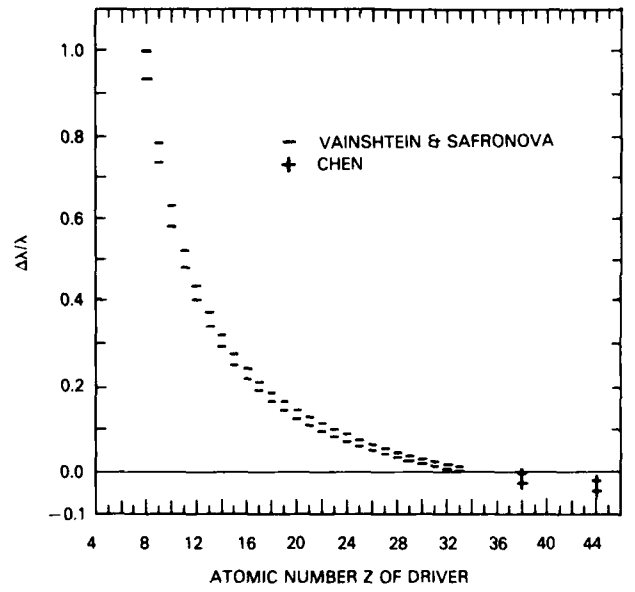

Fig. 18 — Line-matching factor for a Lyman-α pump line from an ion of atomic number Z and a Z-2 Li-like absorber

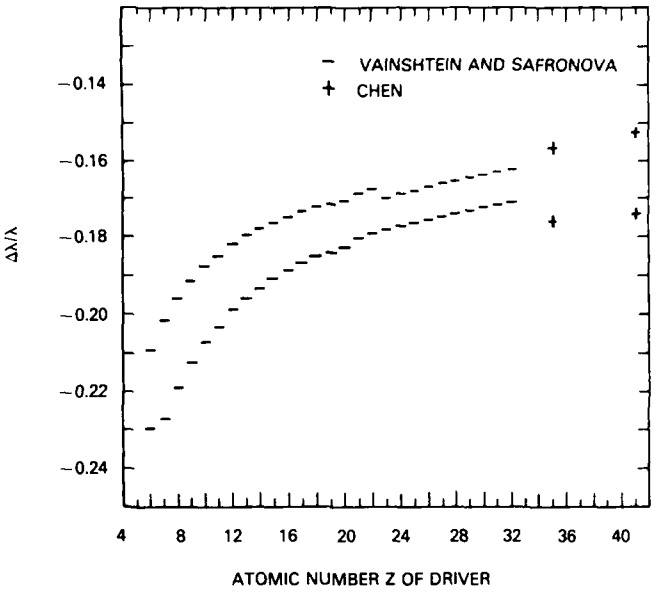

Fig. 19 — Line-matching factor for a Lyman-α pump line from an ion of atomic number Z and a Z+1 Li-like absorber

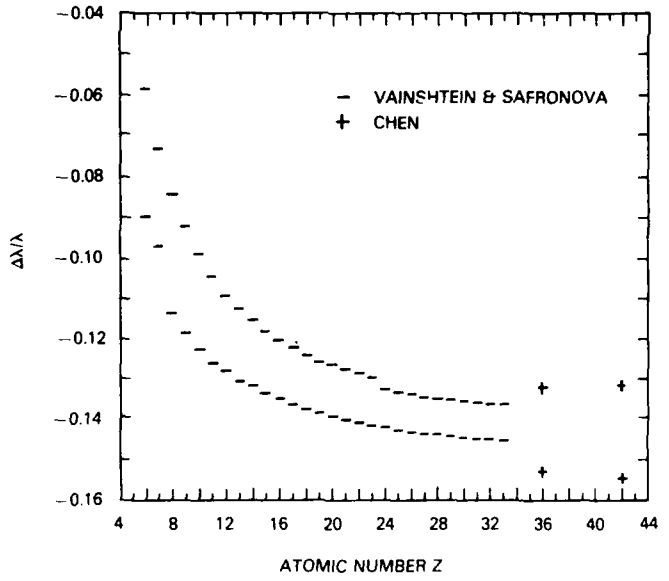

Fig. 20 — Line-matching factor for a Helium-α pump line from an ion of atomic number Z and a Li-like absorber of the same Z

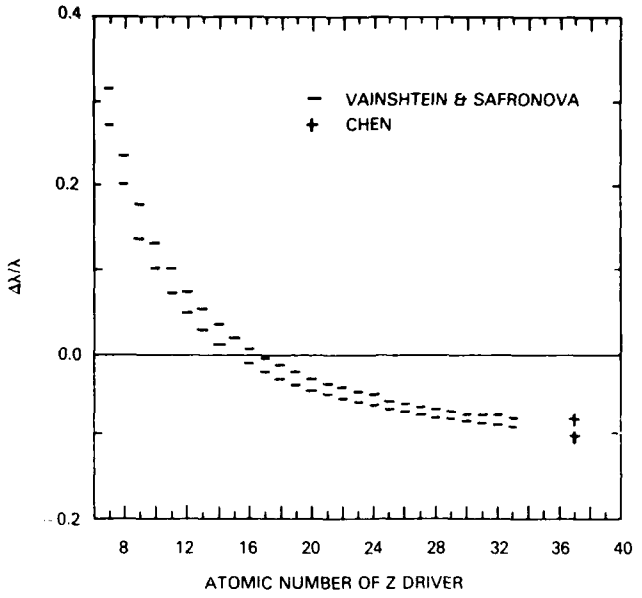

Fig. 21 — Line-matching factor for a Helium-α pump line from an ion of atomic number Z and a Z-1 Li-like absorber

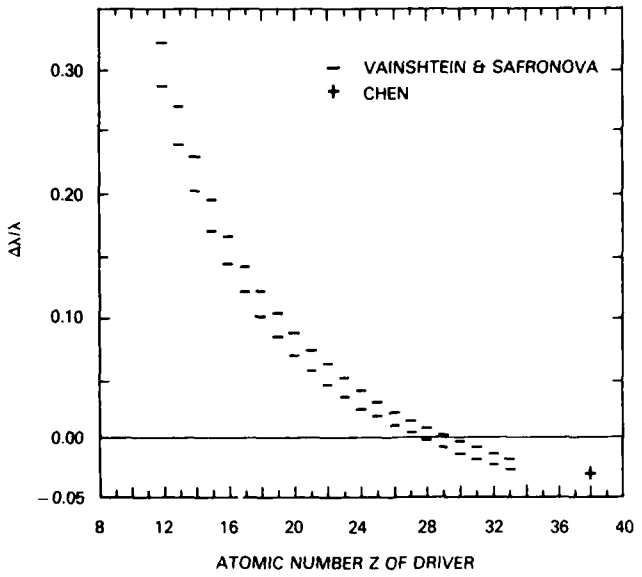

Fig. 22 — Line-matching factor for a Helium-α pump line from an ion of atomic number Z and a Z-2 Li-like absorber

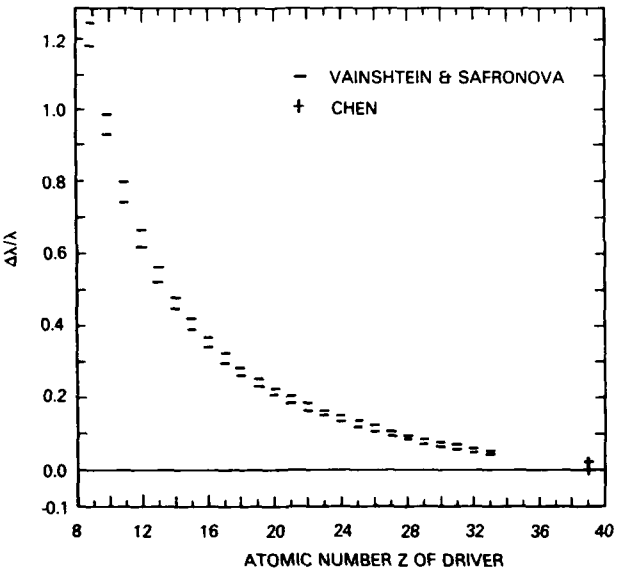

Fig. 23 — Line-matching factor for a Helium-α pump line from an ion of atomic number Z, and a Z-3 Li-like absorber

In the Z_p = 21-23 range for a Lyman-α pump, only one Sc (Z = 21) pumping Ca (Z = 20) transition has both a reasonable wavelength match and a favorable absorption probability and hence is included in Table 2. Matches for a Ti (Z = 22) pump are either B-K transitions with a poor match or B-N transitions with low absorption. For Z = 23, only B-I transitions, ruled out in Table 1, show reasonable matches.

For a Lyman-α pump, Fig. 18 shows that a match with a Z-2 absorber might be possible at Z ~ 35. Absorber data for Z > 33 is published only for Z = 36 and Z = 42, so that no specific matches can be identified in this region [5]. In any case, the wavelength for lasing becomes extremely short (see Fig. 2 or Fig. 3).

For a helium-α pumping ion of nuclear charge Z, Fig. 21 indicates a possible match for a Z-1 absorber in the Z = 15 to 17 range. Table 2 lists an excellent match for S (Z = 16) helium-α pumping P (Z = 15) on a B-M_p, J = 1/2 absorber that appears to satisfy all of the criteria. (Even J = 3/2, the second match shown, is not a bad absorber at a match of $\Delta\lambda/\lambda = 4.8 \times 10^{-4}$.) For Z_p = 28 pumping $Z_a = Z_p$-2 = 26, two matches are shown (Fig. 22). In the first there is a good wavelength match but poor absorption, and just the opposite in the second. Also, for copper Z_p = 29 pumping cobalt $Z_a = Z_p$-2 = 27, there is a good match, but again the absorption is low.

Figure 23 shows that a helium-α Z_p = 40 driver could pump a $Z_a = Z_p$-3 = 37 absorber; however, absorption data for Z_a > 33 is published [5] only for Z_a = 36 (Z_p = 39, as included in Fig. 18) and for Z_a = 42. Hence no match can be identified at present for this combination.

Criterion 8: This requirement calls for a strong laser transition. This is assured by the 3-2 electric dipole transitions chosen.

Criterion 9: This requirement specifies that absorption of the laser emission be kept low for optimum output power. Other than for coincidental line overlaps, natural merges occur for the next lower Z element, in this case, Be-like ions and for very high Z. This is shown first in Fig. 24, where the available wavelength differences between the 3-2 Li-like lasing line [4,5] and 3p-2s, 3s-2p Be-like absorption lines, divided by wavelength, are plotted vs atomic number Z. Extrapolated, this figure indicates an exact overlap at a somewhat higher Z than plotted. The logarithm of the absolute value of this wavelength-decrement ratio is plotted in Fig. 25 and compared with that for Doppler

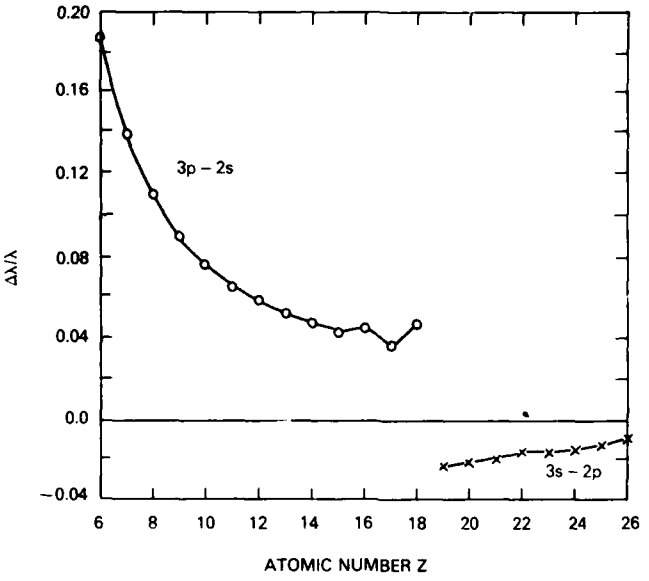

Fig. 24 — Wavelength decrement factor for coincidences between laser emission and 3p-3s, 3s-2p absorption transitions in Be-like ions of the same Z

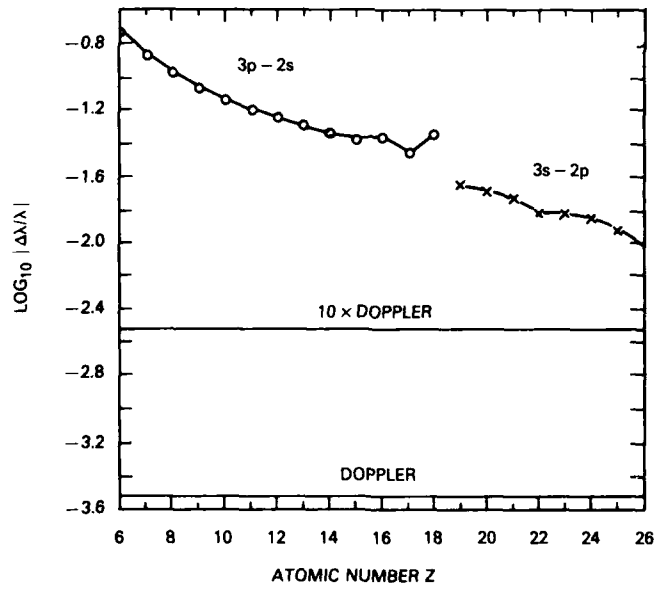

Fig. 25 — Log_{10} of the wavelength decrement factor for coincidences between laser emission and 3p-3s, 3s-2p absorption transitions in Be-like ions of the same Z. Shown are the decrement factors for pure Doppler line spreading (broadening) and for 10 times this, associated with an optical depth of ~ 100.

broadening (3×10^{-4}) as well as 10 times this, which is equivalent to an optical depth of ~ 100 for the Be-like absorbing transition. This indicates that a Doppler absorption coincidence might occur at $\sim Z = 36$ with a very dense absorber of opacity ~ 100, and at a very much higher Z without opacity broadening.

Criterion 10: This requirement addresses the practical need to use two plasma species of close Z, if possible, for similar temperatures, etc. This is met most closely in the case of fluorine in Table 2.

SUMMARY AND RECOMMENDATIONS

We have described a new class of quasi-cw X-ray lasers that are scalable to very short wavelengths and operating on transitions above the normal ionization level. We suggest that the lower laser level decays predominantly by autoionization. The goal is to eliminate quenching due to radiative trapping and hence lead to large-scale X-ray amplifiers. Much systematic effort is needed to make this a reality. The selective matched-line resonant photon pumping proposed needs to be demonstrated, perhaps first on "optical" transitions at short wavelengths. Wavelength matches suggested by calculations need to be verified by accurate photoabsorption measurements on plasma ions, followed by fluorescence experiments, prior to laser demonstrations. Some photoabsorption measurements of doubly excited states in Li-like species at low Z and in neutral [11], singly [11-14], doubly [11,13], and even triply [11] ionized atoms have been performed. Some such transitions are observed also in emission [11]. Autoionization rates are measured also for neutral [15-17] and singly ionized species [18]. Detailed numerical modeling including competing energy levels and collisional mixing is needed, particularly for primary candidates identified by atomic physics experiments.

ACKNOWLEDGMENT

This research was supported by the U.S. Strategic Defense Initiative Office.

REFERENCES

1. R.C. Elton, NRL Memorandum Report 5906, Dec. 1986.

2. R.C. Elton, Proc. X-87 International Conf. on X-Ray and Innershell Processes, *J. de Physique* (in press).

3. J.G. Lunney, *Optics Comm.* **53**, 235 (1985).

4. L.A. Vainshtein and U.I. Safronova, *Atomic Data and Nuclear Data Tables* **25**, 311 (1980).

5. M.H. Chen, *Atomic Data and Nuclear Data Tables* **34**, 301 (1986).

6. F. Bely-Dubau, A. H. Gabriel and S. Volonte, *Mon. Not. R. Astron. Soc.* **186**, 405 (1979).

7. M.H. Chen, private communication, 1987.

8. R.C. Elton, "Atomic Processes", Chapter 4, p. 163 in *Methods of Experimental Physics, Plasma Physics*, H.R. Griem and R.H. Lovberg, eds. (Academic Press, NY, 1970).

9. G.W. Erickson, *J. Phys. Chem. Ref. Data* **6**, 831 (1977).

10. L.S. Vainshtein and U.I. Safronova, *Phys. Scripta* **31**, 519 (1985).

11. E.T. Kennedy and P.K. Carroll, *J. Phys. B*, **11**, 965 (1978).

12. E. Jannitti, P. Nicolosi, G. Tondello, and W. Yongchang, Proc. AIP Topical Conf. on Laser Techniques in the Extreme-UV, Boulder, CO, S.E. Harris and T.B. Lucatorto, eds., AIP Conf. Proc. No. 119, p. 461 (1984).

13. E. Jannitti, P. Nicolosi, and G. Tondello, *Physics* **124C**, 139 (1984).

14. E. Jannitti, M. Mazzoni, P. Nicolosi, G. Tondello and W. Yongchang, *J. Opt. Soc. Am.* **2**, 1078 (1985).

15. S. Mannervik, *Phys. Scripta* **22**, 575 (1981).

16. H. Cederquist and S. Mannervik, *J. Phys. B*, **15**, L807 (1982).

17. H. Cederquist and S. Mannervik, *Phys. Rev. A* **31**, 171 (1985).

18. H. Cederquist, M. Kisielinski, S. Mannervik, and T. Anderson, *J. Phys. B*, **17**, 1969 (1984).

END

DATE

FILMED

9-88

DTIC